Available online at www.sciencedirect.com
SCIENCE DIRECT®
Chemical Physics Letters 397 (2004) 82–86
www.elsevier.com/locate/cplett

An investigation of the HOMO electron density distribution of cyclopentene by electron momentum spectroscopy ☆

X.G. Ren, C.G. Ning, J.K. Deng *, S.F. Zhang, G.L. Su, H. Zhou, B. Li, G.Q. Li

Department of Physics, Tsinghua University, Beijing 100084, PR China

Received 28 July 2004; in final form 19 August 2004
Available online 12 September 2004

Abstract

The highest occupied molecular orbital (HOMO) of cyclopentene (C_5H_8) has been studied by a binary (e, 2e) electron momentum spectroscopy, at an impact energy of 1200 eV plus the binding energy and using symmetric non-coplanar kinematics. The first measurements of the complete valence shell binding energy spectra and the HOMO momentum profile are reported. The experimental momentum profile of HOMO is compared with the theoretical momentum profiles calculated using Hartree–Fock and density functional theory method with various basis sets. The EMS experimental result is well described by the calculations.

1. Introduction

Organic-semiconductor hybrid materials provide a favorable linking of organic chemistry to existing semiconductor based microelectronic technologies, therefore the interaction of organic molecules with surface represents an area of significant scientific and technological interest because of its importance in surface chemistry. The cyclopentene, also known as cyclopenten, C_5H_8 is widely used in this kind of organic-semiconductor surface chemistry reaction [1,2]. The cyclic unsaturated hydrocarbons such as cyclopentene [1,2], cyclohexene [1], 1,4-cyclohexadine [3], 1,3-cyclohexadine, 1,3,5,7-cyclooctatetraene [4] and 1,5-cyclooctadiene [5] have been used for the fabrication of ordered organic monolayer films on semiconductor surfaces and form the cycloaddition products. These hybrid organic-semiconductor systems are promising for the development of molecular electronics because of the possibility of combining the wide range of functionality of organic molecules with the existing semiconductor based infrastructure. According to experimental [1] and theoretical [2] studies, the cyclic unsaturated hydrocarbons can react with the semiconductor surface through interaction between the C=C double bonds of the hydrocarbon and the dangling bonds of a semiconductor dimer. The highest occupied molecular orbital (HOMO) of cyclopentene possesses the C=C π bond character [6]. In the reaction chemistry the HOMO of the reactant molecules such as cyclopentene plays a determining role in directing chemical reactivity [7,8]. Therefore the useful properties of the cyclic unsaturated cyclopentene such as molecule structure, binding energies, momentum profile and orbital electron density distribution of the HOMO C=C bond can provide some significant information for the adsorption or dehydrogenation reaction of cyclopentene with semiconductor surface.

Electron momentum spectroscopy (EMS), also known as binary (e, 2e) spectroscopy, is an electron impact ionization process [9–11]. EMS measurements and

☆ Project supported by the National Natural Science Foundation of China under Grant Nos. 19854002, 19774037 and 10274040 and the Research Fund for the Doctoral Program of Higher Education under Grant No. 1999000327.
* Corresponding author. Fax: +861 062 781604.
E-mail address: djk-dmp@mail.tsinghua.edu.cn (J.K. Deng).

0009-2614/$ - see front matter © 2004 Elsevier B.V. All rights reserved.
doi:10.1016/j.cplett.2004.08.093

high level quantum mechanical calculations provide very detailed information on the binding energies, momentum profiles and orbital electron density distributions of atoms and molecules. The unique ability of EMS to measure electron momentum distributions of individual molecular orbital has made it become an important technique of experimental electronic structure studies of atoms, molecules and solids [11]. Furthermore, since electron momentum profile is sensitive to diffuse parts of the position wave function, EMS can provide information relevant to issues of chemical reaction and molecular recognition, and the momentum-space electron density may be a criterion for molecular similarity and dissimilarity [12]. In this Letter, we report the first complete valence shell binding energy spectra (2–34 eV) of cyclopentene C_5H_8 and the HOMO electron momentum profile measurements using EMS at an impact energy of 1200 eV plus binding energy and using symmetric non-coplanar geometry. Our experimental momentum profile (XMP) is compared with Hartree–Fock (HF) and density functional theory (DFT) calculation using various basis sets.

2. EMS theoretical background

In the EMS experiment the relative (e, 2e) cross-section for electron impact ionization (i.e. the binary (e, 2e) reaction) is measured by detecting the two outgoing electrons in coincidence. The particular kinematics of the experiment is chosen in such a way as to provide a straightforward relation between some variable kinematics parameters and the momentum of the ionized electron prior to knock-out. For this purpose the symmetric non-coplanar kinematics [9–11] is the most convenient and frequently used experimental configuration. In this (e, 2e) kinematics the target molecules are ionized by a beam of electrons, and the two outgoing electrons have equal polar angles $\theta(\theta_1 = \theta_2 = 45°)$ relative to the incoming electron beam. The relative azimuthal angle ϕ between the two outgoing electrons is varied by rotating one of the analyzers over a range of angles around the incident beam axis. This procedure essentially provides a measurement of the electron momentum distribution at a given binding energy, since the azimuthal angle ϕ is related to the momentum p of the ionized electron prior to impact by the formula [9–11]

$$p = \left[(2p_1 \cos\theta - p_0)^2 + \left(2p_1 \sin\theta \sin\left(\frac{\phi}{2}\right)\right)^2 \right]^{1/2}, \quad (1)$$

where p_1 and p_0 are the momenta of the outgoing and incident electrons, respectively. If the incident electron energy is varied, a binding energy spectrum (BES) can be recorded at each azimuthal angle ϕ. The binding energy selectivity of EMS permits the probing of individual orbital of the total many-electron wave function. Variation of ϕ at a given binding energy therefore yields an orbital momentum (density) distribution.

The EMS reaction theory is based on several approximations [9–11] through which the (e, 2e) cross-section is related to the electronic structure. Of these the most important are the binary encounter approximation and the plane-wave impulse approximation. In order to ensure the validity of these approximations the experiment has to be conducted under what are known as EMS conditions, which are sufficiently high electron impact energy (typically 1200 eV plus the binding energy for valence electrons) and, optimally, the use of the symmetric non-coplanar kinematics. Under these EMS conditions the kinematics factors are effectively constant, the EMS cross-section for randomly oriented molecules can be given [11,13] by

$$\sigma_{\mathrm{EMS}} \propto \int \mathrm{d}\hat{p} |\langle p\Psi_f^{N-1} || \Psi_i^N \rangle|^2, \quad (2)$$

where p is the momentum of the target electron prior to electron ejection. $|\Psi_f^{N-1}\rangle$ and $|\Psi_i^N\rangle$ are the total electronic wave functions for the final ion state and the target molecule ground (initial) state, respectively. The integral represents the spherical average due to the randomly oriented gas phase target in the collision region [11]. The overlap of the ion and neutral wave functions in Eq. (2) is known as the Dyson orbital while the square of this quantity is referred to as an ion-neutral overlap distribution (OVD). Thus, the (e, 2e) cross-section is essentially proportional to the spherical average of the square of the Dyson orbital in momentum space [9–11].

Eq. (2) is greatly simplified by using the target Hartree–Fock approximation (THFA). Within the THFA, only final (ion) state correlation is allowed and the many-body wave functions $|\Psi_f^{N-1}\rangle$ and $|\Psi_i^N\rangle$ are approximated as independent particle determinants of ground state target HF orbital. In this approximation Eq. (2) is reduced to

$$\sigma_{\mathrm{EMS}} \propto \int \mathrm{d}\Omega |\Psi_j(p)|^2, \quad (3)$$

where $|\Psi_j(p)\rangle$ is the one-electron momentum space canonical HF orbital wave function for the jth electron, corresponding to the orbital from which the electron was ionized. The probability of the ionization event producing a one-hole configuration of the final ion state. The quantity $|\Psi_j(p)\rangle$ is the Fourier transform of the more familiar one-electron position space orbital wave function $|\Psi_j(r)\rangle$. The integral in Eq. (3) is known as the spherically averaged one-electron momentum distribution (MD). Thus, EMS has the ability to image the electron density distribution in individual orbital selected according to their binding energies [9–11].

The Kohn–Sham DFT provides the alternative approach to approximating the Dyson Orbital in Eq. (2). The target Kohn–Sham approximation (TKSA) has been shown to give a good description of the XMPs of lots of molecules measured by EMS [11]. The TKSA gives a result similar to Eq. (3) with the canonical HF orbital replaced by a momentum space Kohn–Sham orbital (KSO) $|\Psi_j^{\mathrm{KS}}(p)\rangle$,

$$\sigma_{\mathrm{EMS}} \propto \int \mathrm{d}\Omega |\Psi_j^{\mathrm{KS}}(p)|^2. \tag{4}$$

It should be noted that accounting of electron correlation effects in the target ground state is included in the TKSA via the exchange correlation potential. A more detailed description of the TKSA–DFT method may be found elsewhere [14].

3. Experimental background of EMS

In this work the experiment is carried out using an energy dispersive multichannel electron momentum spectrometer, for which the details of construction and operation have been reported earlier [15]. Briefly, the target molecules are ionized by a beam of electrons with an impact energy of 1200 eV plus the binding energy, and the two outgoing electrons are selected at equal polar angles relative to the direction of the incident electron beam. The two outgoing electrons are energy-analyzed by hemispherical analyzers and detected in coincidence using time-correlated position-sensitive microchannel plate detectors in the energy dispersive exit planes of the analyzers. One analyzer can be rotated around the beam axis over a range of relative azimuthal angles ϕ from 0° (coplanar position) to ±30°. The electron coincidence counts are recorded at each ϕ value as the impact energy is varied and this procedure results in a series of angularly resolved BES.

The XMPs were obtained by fitting the experimental BES at each azimuthal angle with an appropriate set of bands and then converting the angular dependence of the area under each band into the momentum distribution by using Eq. (1). To compare the XMPs with the relative cross-sections calculated as a function of momentum using Eqs. (2)–(4), the effects of the finite spectrometer acceptance angles in both θ and ϕ ($\Delta\theta = 0.6°$ and $\Delta\phi = 1.2°$) must be included in the calculations. After momentum resolution folding, the OVD (Eq. (2)) or the MD (Eq. (3) or Eq. (4)) is referred to as a theoretical momentum profiles (TMPs). 12 binding energy spectra over the energy range of 2–34 eV were collected at the out-of-plane azimuthal angles ϕ, 0°, 1°, 2°, 3°, 4°, 6°, 8°, 10°, 12°, 14°, 17° and 22° in a series of sequential repetitive scans.

4. Results and discussions

Cyclopentene (C_5H_8) has C_s point group symmetry according to molecular orbital theory. Its ground state electronic configuration can be written as

$$(\mathrm{Core})^{10}\underbrace{(1a')^2(2a')^2(1a'')^2(3a')^2}_{\mathrm{InnerValence}}\underbrace{(2a'')^2(4a')^2(5a')^2(3a'')^2(6a')^2(7a')^2(4a'')^2(8a')^2(5a'')^2(9a')^2}_{\mathrm{OuterValence}}.$$

In the ground state, the 38 electrons are arranged in 19 double-occupied orbitals in the independent particle description. All the molecular orbitals are either a′-type or a″-type. There is no degeneracy in these orbitals. The assignment of the order of occupation for these valence orbitals, both from PES experiments and from molecular orbital calculations, has been discussed in [6,16,17].

The calculations of cyclopentene have been carried out at the ab initio level, using the GAUSSIAN 98W program together with the HEMS program developed by UBC. In order to compare with the XMPs, the instrumental angular (momentum) resolution was incorporated in all the calculations using the UBC RESFOLD program based on the Gaussian weighted planar grid (GWPG) method [18].

The valence shell BES of cyclopentene for measurements at azimuthal angle $\phi = 1°$ and $\phi = 8°$ are shown in Fig. 1. The binding energy spectra were fitted with a series of individual Gaussian peaks. The relative energy values were given by the ionization potentials determined by high-resolution PES [6,17,19]. The widths of Gaussian peaks are combinations of EMS instrumental energy resolution and Frank–Condon widths of the corresponding bands determined by high-resolution PES [6,17]. In Fig. 1 Gaussian peaks fitted to the individual transitions are shown by dashed lines while their sums are represented by the solid line.

The PES spectrum of the outer valence orbitals region has been reported in [6] using He I radiation source. In the PES work, the vertical ionization potential of the 9a′ HOMO was 9.18 eV. And the 5a″, 8a′, 4a″, 7a′, 6a′, 3a″, 5a′ and 4a′ orbitals were determined to be 11.6, 12.0, 12.2, 12.6, 13.1, (14.0), 15.8 and 16.1 eV, respectively. Another PES studies of cyclopentene were reported by Wiberg et al. [17] using He I and He II radiation source which included some of the inner valence region of C_5H_8 and the ionization potential of the 9a′ HOMO was 9.20 eV. And the 5a″, 8a′, 4a″, 7a′, 6a′, 3a″, 5a′, 4a′ and 2a″ orbitals were determined to be 11.6, 12.0, 12.2, 12.6, 13.08, 14.0, 15.8, 16.1 and 17.3 eV, respectively. In the inner valence region the vertical ionization potential of 3a′ orbital was 19.0 eV. The average vertical ionization potential of the 2a′ and 1a″ orbitals was 22.0 eV. The ionization potential at 26.0 eV was assigned to the innermost valence 1a′ orbital by Streets and Potts [19].

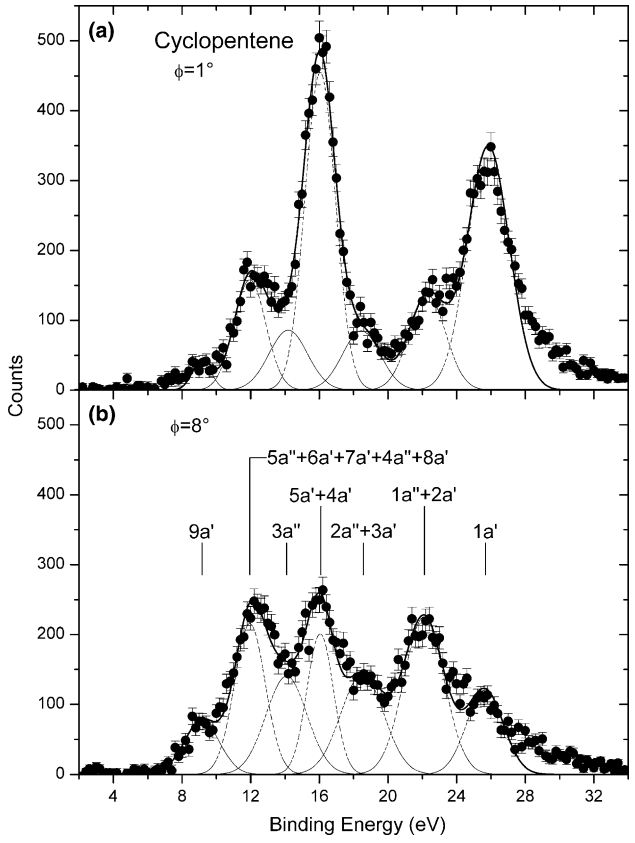

Fig. 1. Binding energy spectra of cyclopentene at $\phi = 1°$ (a) and $\phi = 8°$ (b). The dashed and solid lines represent individual and summed Gaussian fits, respectively.

In our EMS work, seven structures can be identified in the binding energy spectra of Fig. 1. The vertical ionization potential of HOMO 9a′ is determined to be 9.15 eV. The averaged vertical ionization potentials of the (5a″ + 8a′ + 4a″ + 7a′ + 6a′), 3a″ and (5a′ + 4a′) are determined to be 11.95, 14.19 and 16.05 eV, respectively. The 3a″ orbital is considered as an individual state in our EMS binding energy spectra, because a large discrepancy and uncertainty in the adjacent bands will be emerged without considering the individual 3a″ state in the curve fitting process. Another evidence of the individual 3a″ state can be given from the PES data [6,17]. The averaged ionization potentials of (2a″ + 3a′), (2a′ + 1a″) and 1a′ inner valence orbitals were determined to be 18.30, 22.30 and 25.85 eV, respectively. In addition, some rather weak satellite structures due to many-body correlation effects in the target or in the residual ion final states are also observed above 26.0 eV in the binding energy spectra. The differences in FWHM are due to the vibrational broadening of the lines. The binding energy values in Fig. 1 are consistent with the PES data [6,17,19].

EMS measurement of cyclopentene HOMO 9a′ XMP has been extracted by deconvolution of the same peak from the sequentially obtained binding energy spectra at different azimuthal angles, and therefore the relative normalization for the different transitions are maintained. The XMP is compared, in Fig. 2, with the TMPs within the THFA or TKSA using the HEMS program. The canonical HF orbitals for cyclopentene are calculated using the STO-3G, 4-31G, 6-31G, 6-311++G** and AUG-CC-PVTZ basis sets. The Kohn–Sham orbitals are obtained by running DFT calculations utilizing the B3LYP hybrid gradient functional, with the 6-311++G** and AUG-CC-PVTZ basis sets. The TMPs were folded with the finite instrumental angular (momentum) resolution using the RESFOLD program to account for the spectrometer resolution.

The TMPs for the HOMO calculated within the THFA as well as the TKSA and the experimental results are also shown in Fig. 2. The experimental results are normalized to the B3LYP/AUG-CC-PVTZ calculation for the HOMO. It can be seen from Fig. 2 that Hartree–Fock calculations with small basis set (6-31G, 4-31G and STO-3G shown by curves 5, 6 and 7, respectively) give rather poor predictions of the HOMO XMP, especially in the low p region below 1.0 a.u. The 6-311++G** and AUG-CC-PVTZ HF calculations (curves 1 and 2 in Fig. 2) give a somewhat better quantitative fit to the experimental results than the small basis set calculations in the low p region below 0.3 a.u.. Using these two improved basis sets a better quantitative agreement with experiment is then achieved using the DFT-B3LYP calculations with AUG-CC-PVTZ basis set (Curve 4). The better performance of the gradient corrected DFT method with AUG-CC-PVTZ basis set compared with the corresponding HF treatments indicates that inclusion of dynamic electron correlation effects method with the saturated diffuse and Dunning's correlation consistent polarization basis set calculation

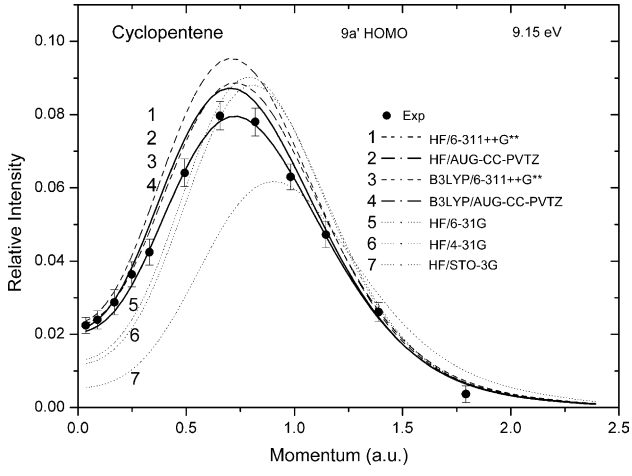

Fig. 2. Experimental and calculated momentum distributions for 9a′ HOMO of cyclopentene. The TMP were calculated using HF and DFT-B3LYP methods with various basis sets.

is essential for modeling the chemically important larger r (lower p) region of the HOMO of cyclic unsaturated hydrocarbon cyclopentene.

5. Summary

In summary, the first measurements of the complete valence binding energy spectra and electron density distribution for C_5H_8 HOMO are reported in this Letter. The presently reported EMS data indicate that for the HOMO of cyclopentene a calculated electron momentum density distribution by DFT method with AUG-CC-PVTZ basis set give a better description of the XMP. The DFT method using generalized gradient functionals with saturated diffuse and Dunning's correlation consistent polarization basis set provides an accurate method including electron correlation effects into quantum chemical calculations for the cyclic C_5H_8 HOMO electron momentum distribution. Our experimental results and related theoretical calculations provide a very good description of the cyclopentene HOMO Dyson Orbital density, i.e. how an electron is transferred out of the molecule. Therefore the adsorption or cycloaddition reaction of cyclopentene with semiconductor surface, since the HOMO is particularly important for chemical reactivity and possibly molecular recognition from the pioneering work by Fukui on frontier orbital theory [8], may increasingly benefit from the experimental and theoretical electron density distribution of the HOMO of cyclopentene.

Acknowledgements

The authors acknowledge the help of Professor Zhu Qihe.

References

[1] S.W. Lee, J.S. Hovis, S.K. Coulter, et al., Surf. Sci. 462 (2000) 6.
[2] J.H. Cho, L. Kleinman, Phys. Rev. B 65 (2002) 245407.
[3] J.H. Cho, D.H. Oh, K.S. Kim, L. Kleinman, J. Chem. Phys. 116 (2002) 3800.
[4] J.S. Hovis, R.J. Hamers, J. Phys. Chem. B 102 (1998) 687.
[5] J.S. Hovis, R.J. Hamers, J. Phys. Chem. B 101 (1997) 9581.
[6] K. Kimura, S. Katsumata, Y. Achiba, T. Yamazaki, S. Iwata, Handbook of He I Photoelectron Spectra of Fundamental Organic Molecules, Japan Scientific Society, Tokyo, 1981.
[7] C.E. Brion, G. Cooper, Y. Zheng, et al., Chem. Phys. 270 (2001) 13.
[8] K. Fukui, The Role of Frontier Orbitals in Chemical Reaction in Les Prix Nobel ca. 1981, The Nobel Foundation, 1982.
[9] I.E. McCarthy, E. Weigold, Rep. Prog. Phys. 54 (1991) 789.
[10] C.E. Brion, Int. J. Quantum Chem. 29 (1986) 1397.
[11] E. Weigold, I.E. McCarthy, Electron Momentum Spectroscopy, Kulwer, New York, 1999.
[12] D.L. Cooper, N.L. Allan, J. Am. Chem. Soc. 114 (1992) 4773.
[13] K.T. Leung, C.E. Brion, Chem. Phys. 82 (1983) 87.
[14] P. Duffy, D.P. Chong, M.E. Casida, D.R. Salahub, Phys. Rev. A 50 (1994) 4704.
[15] J.K. Deng, G.Q. Li, Y. He, et al., J. Chem. Phys. 114 (2001) 882.
[16] N. Naga, Y. Imanishi, Polymer 43 (2002) 2133.
[17] K.B. Wiberg, G.B. Ellison, J.J. Wendoloski, et al., J. Am. Chem. Soc. 98 (1976) 7179.
[18] P. Duffy, M.E. Casida, C.E. Brion, D.P. Chong, Chem. Phys. 159 (1992) 347.
[19] D.G. Streets, A.W. Potts, J. Chem. Soc., Faraday Trans II 70 (1974) 1505.